ACS Catalysis

Research Article

pubs.acs.org/acscatalysis

Oxygen Reduction at a Cu-Modified Pt(111) Model Electrocatalyst in Contact with Nafion Polymer

Jakub Tymoczko,[†] Federico Calle-Vallejo,[‡] Viktor Colic,[†] Marc T. M. Koper,[§] Wolfgang Schuhmann,[†] and Aliaksandr S. Bandarenka*[,†,∥]

[†]Analytical Chemistry-Center for Electrochemical Sciences (CES), Ruhr-Universität Bochum, Universitätsstrasse 150, 44780 Bochum, Germany

[‡]Laboratoire de Chimie, ENS Lyon, Université de Lyon, CNRS, 46 Allée d'Italie, 69364 Lyon Cedex 07, France

[§]Leiden Institute of Chemistry, Leiden University, P.O. Box 9502, 2300 RA Leiden, The Netherlands

[∥]Physik-Department ECS, Technische Universität München, James-Franck-Strasse 1, D-85748 Garching, Germany

ABSTRACT: The effect of Nafion on the performance of a model Cu-modified Pt(111) electrocatalyst has been investigated using electrochemical techniques and density functional theory calculations. In this work, we demonstrate that Cu subsurface alloying not only increases the activity of model Pt(111) electrodes toward the oxygen reduction reaction (ORR) but also largely prevents catalyst poisoning by electrolyte components relevant for polymer electrolyte membrane fuel cell applications. Our results indicate that specific adsorption of (bi)sulfates and sulfonates (present in Nafion membranes) on the Cu-modified Pt(111) electrocatalyst is gradually suppressed, which implies that the ORR activity in 0.05 M H_2SO_4 electrolyte drastically increases, with a change in the corresponding pseudo-half-wave potential of ~93 mV. Importantly, the Cu-modified Pt(111) electrocatalyst in contact with Nafion polymer shows an activity as high as that in the absence of this polymer in perchloric acid media.

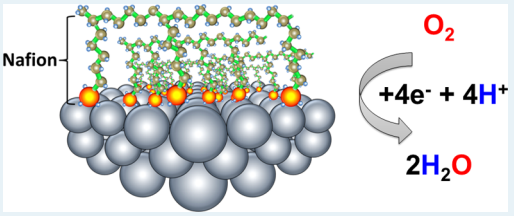

KEYWORDS: *(bi)sulfate adsorption, Pt(111) single crystals, near-surface alloys, electrocatalysis, Nafion*

1. INTRODUCTION

Efforts dedicated to the optimization of catalyst performance with respect to the oxygen reduction reaction (ORR) are closely related to the growing demand for clean, sustainable, and renewable energy conversion devices, for instance, polymer electrolyte membrane fuel cells (PEMFCs).[1,2] As a consequence, understanding the properties of the electrolyte/electrode interface as well as the mechanistic aspects of adsorption processes at these interfaces constitutes an important research area in electrocatalysis and PEMFC technology.[3,4] In the past, research on Pt alloyed with the 3d transition metals (Cu, Ni, Fe, Co, etc.) has received increased amount of attention because of its significantly improved electrocatalytic activity toward the ORR in acidic electrolyte environments.[5−10] Generally, single-crystal electrodes in model electrolytes are commonly used to establish a correlation between the surface (or interfacial) properties of the material and its electrocatalytic performance. However, the transition from such model systems to real devices is not always straightforward. For instance, the so-called membrane electrode assembly (MEA), which is one of the key elements in PEMFCs, is a significantly more complex system; findings obtained using model electrodes and electrolytes cannot often be directly used to design real-world catalytic systems. MEAs normally consist of an ion-conducting solid polymer electrolyte (typically Nafion) placed in the proximity of the electrocatalytic surface embedded in an interpenetrating network of electronic conductors.[11] In this case, it is well accepted that the performance of PEMFCs would strongly depend on the catalyst loading, the electronic structure of the catalyst surface, and the number of active sites available for the ORR. In contrast to the numerous studies and profound understanding of the possible strategies for optimization of the catalyst performance in some model electrolytes (e.g., in perchloric acid), relatively little is known about the true effect of Nafion on the performance of active Pt-based catalysts alloyed with transition metals.

Recently, specific interactions between Nafion and Pt surfaces have been extensively investigated using cyclic voltammetry and the CO-displacement method. For example, Subbaraman et al.[12] have found that Nafion electrolyte components, particularly sulfonate groups, adsorb specifically on Pt(111). Additionally, recent studies showed that the adsorption of oxygenated species (OH_{ad}) at 0.8 V in 0.1 M $HClO_4$ on state-of-the-art Pt(111) and $Pt_3Ni(111)$ catalysts is dramatically affected by competing adsorption of anionic species from Nafion. Consequently, the electrocatalytic activity toward the oxygen reduction reaction for both Pt(111) and $Pt_3Ni(111)$ decreases by ~25% in the presence of this sulfonated proton-conducting polymer.[13] The knowledge

Received: July 20, 2014
Revised: September 9, 2014
Published: September 9, 2014

 © 2014 American Chemical Society

obtained during these studies has significantly helped to assess the nature of adsorbed species and establish relationships between some interfacial properties and electrocatalytic activity toward the ORR in the presence of Nafion; the current understanding is, nonetheless, far from sufficient.

To prevent the deactivation of the ORR catalysts in the presence of Nafion, Shinohara et al.[14] developed an ionomer consisting of two sulfonimide acid groups in its side chain ending with a hydrophobic group, instead of a sulfonic acid group. This modification resulted in a proton conductivity and an oxygen permeability higher than those of Nafion. It was also expected to be "less poisonous" with a beneficial influence on the ORR kinetics due to a stronger steric effect hindering anion co-adsorption. However, cyclic voltammetry experiments showed that the co-adsorption of anions still existed and could not be sufficiently prevented by means of this strategy.

Selective positioning of monolayer amounts of foreign atoms at the surface and subsurface regions of metal electrodes is a promising way to optimize the properties of the electrode/electrolyte interface.[15,16] In our recent study, we demonstrated that the relative position of Cu atoms at the surface drastically changes the adsorption energies for (bi)sulfate anions at the Pt(111) interface.[17] Here, we focus on the adsorption of anionic species present in Nafion membranes on Pt(111) and Cu/Pt(111) near-surface alloy (NSA) electrodes and their influence on the ORR kinetics. We show that monolayer amounts of Cu in the subsurface region of Pt(111) electrodes can be efficiently used to simultaneously improve the ORR electrocatalytic activity of Pt(111) in the presence of co-adsorbing (bi)sulfate anions and largely mitigate the negative influence of the Nafion polymer ionic functional groups.

2. EXPERIMENTAL AND COMPUTATIONAL DETAILS

Before the experiments, all glassware was cleaned in a 50% HF aqueous solution followed by multiple rinses with Siemens ultrapure water. All model experiments were performed using two Pt(111) single crystals with diameters of 5 mm, oriented better than 0.1° (Mateck, Jülich, Germany). Details of the preparation and electrochemical characterization of Pt(111) single-crystal surfaces and Cu/Pt(111) near-surface alloys (NSAs) have been described previously.[18,19] Briefly, to prepare the NSAs, a specially designed cell for the controllable thermal treatment and electrochemical characterization of single-crystal alloy electrodes was used.[19,20] A monolayer (ML) of Cu was initially deposited on the Pt(111) electrode using electrochemical underpotential deposition (UPD).[21] For that, the electrode potential was held at 0.33 V versus a reversible hydrogen electrode (RHE) for 3 min in 0.1 M $HClO_4$ electrolyte containing 2 mM Cu^{2+}. Afterward, the electrode was rinsed with ultrapure water (under potential control), dried, and annealed under a reducing Ar/H_2 (5%) atmosphere at 400 °C for 2 min. While the theoretical analysis suggests the maximal amount of Cu in the second Pt layer to be 1 ML, this procedure results in samples with a subsurface concentration of Cu of $\sim^2/_3$ ML, as was found recently.[37] Further issues related to the electrochemical stability of the Cu/Pt(111) NSAs have been discussed elsewhere.[18,22,37]

Nafion-coated electrodes were prepared by dropping 10 μL of a Nafion solution on the electrode. The Nafion solution was prepared by diluting a 5 wt % Nafion 117 suspension [in a mixture of lower aliphatic alcohols and water (Sigma-Aldrich)] with ultrapure water (1 mL of Nafion in 100 mL of H_2O). The typical drying time was overnight in an Ar atmosphere at room temperature. Aqueous 0.1 M $HClO_4$ (Merck, Suprapur) and 0.05 M H_2SO_4 (Merck, Suprapur) solutions were used as working electrolytes. All potentials are referred to the RHE scale. Pt(111) working electrodes were heated under controlled atmospheres using an inductive heater with an automatic time controller (20−80 kHz, 15KW-EQ-SP-15A, MTI). O_2, Ar (5.0, Air Liquide), and Ar/H_2(5%) (6.0, Air Liquide) pure gases and gas mixtures were used in all experiments. A Biologic SP-300 potentiostat was used to perform cyclic voltammetry and rotating disk electrode (RDE) experiments. All experiments were performed at room temperature (21 ± 1 °C).

Density functional theory (DFT) calculations were performed with the VASP code,[23] using the PBE exchange correlation functional[24] and PAW potentials.[25] Geometry optimizations were made with slabs composed of four metal layers, the two topmost of which and the adsorbates were free to move in all directions. We used the quasi-Newton scheme for the relaxations until the residual force on any atom was below 0.01 eV $Å^{-1}$. We simulated 2 × 2 (111) slabs with 6 × 6 × 1 k-point meshes, which ensured convergence of the adsorption energies within 0.05 eV. At least 12 Å of vacuum was added between periodically repeated images, and dipole corrections were used. The plane-wave cutoff was 450 eV. The Methfessel−Paxton method was used to smear the Fermi level[26] with a k_BT values of 0.2 eV, and all energies were extrapolated to 0 K. The gas phase references (H_2, H_2O, and H_2SO_4) were calculated in boxes of 15 Å × 15 Å × 15 Å, k_BT = 0.001 eV, and a γ-point distribution. The total enthalpies are approximated as follows: $H = E_{DFT}$ + ZPE, where E_{DFT} and ZPE are the total and zero-point electronic energies, respectively, calculated via DFT. The ZPEs in electronvolts for H_2, H_2O, H_2SO_4, *OH, and $*SO_4$ were 0.27, 0.57, 1.02, 0.31, and 0.46, respectively. The DFT energies of adsorption of *OH and $*SO_4$ are given by the following schemes:

$$* + H_2O \rightarrow *OH + \frac{1}{2}H_2 \quad \text{(R1)}$$

$$* + H_2SO_4 \rightarrow *SO_4 + H_2 \quad \text{(R2)}$$

The adsorption configurations on Pt(111) and Cu/Pt(111) NSAs were atop for *OH (following previous results from ref 37) and tridentate on 3-fold hollow sites for $*SO_4$ (following previous results from ref 27). As a first approximation, water solvation and $*OH/*SO_4$ co-adsorption effects were not taken into account.

We consider *O, *OH, and *OOH to be the adsorbed intermediates of the ORR.[28] Note that, as *O, *OH, and *OOH bind through an oxygen atom to catalytic surfaces, linear scaling relations exist among the adsorption energies of those three species.[29,30] Such scaling relations are as follows:

$$\Delta E_O = m_1 \Delta E_{OH} + b_1 \quad (1)$$

$$\Delta E_{OOH} = m_2 \Delta E_{OH} + b_2 \quad (2)$$

The slopes in these scaling relations depend on the number of electrons that the oxygen atoms bound to the surface lack to fulfill the octet rule. The binding oxygen in *OH and *OOH lacks a single electron, whereas it lacks two electrons in *O. Thus, $m_1 = 2/1 = 2$ and $m_2 = 1/1 = 1$. When the adsorption energies of *OH are weakened by the presence of Cu, those of *O and *OOH are expected to be shifted accordingly. As will be shown later, the maximal difference between the adsorption energies of *OH in this study is 0.37 eV. Thus, we expect the

dx.doi.org/10.1021/cs501037y | ACS Catal. 2014, 4, 3772−3778

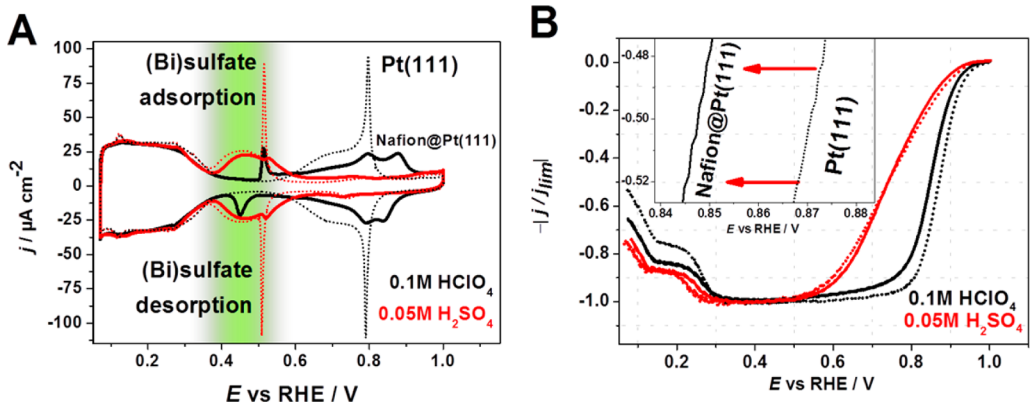

Figure 1. (A) Cyclic voltammograms and (B) anodic parts of RDE polarization curves (iR-corrected) characterizing the bare Pt(111) (···) and Nafion-modified Pt(111) electrodes (—) in (A) Ar-saturated and (B) O_2-saturated 0.1 M $HClO_4$ (black) and 0.05 M H_2SO_4 (red) electrolytes, as indicated, at 1600 rpm. dE/dt = 50 mV/s.

corresponding differences in *O and *OOH adsorption energies to be ∼0.74 and ∼0.37 eV, respectively. The fact that the adsorption energies of *O, *OH, and *OOH scale linearly is what allows volcano-type activity plots to be drawn in terms of a single parameter, namely one of such adsorption energies or a linear combination of them.[31,32]

3. RESULTS AND DISCUSSION

We start our discussion with the effect of the relevant electrolyte components on the adsorption of one of the important ORR intermediates, *OH, and subsequently on the resulting ORR activity. Figure 1 shows corresponding voltammograms for Nafion-free and Nafion-modified Pt(111) electrodes in 0.1 M $HClO_4$ and 0.05 M H_2SO_4. Cyclic voltammetry in O_2-free perchloric acid solutions is often used as a very sensitive tool to evaluate the status and quality of the Pt(111) surface.[33] Generally, three separate regions can be clearly distinguished: (i) the hydrogen adsorption/desorption region between 0.05 and ∼0.35 V, (ii) the double-layer region between ∼0.35 and ∼0.55 V, and (iii) the *OH adsorption/desorption region (where an asterisk denotes adsorbed species) between approximately 0.55 and 0.8 V. The height and sharpness of the "butterfly" peaks at approximately 0.8 V are commonly used to assess the surface quality of Pt(111) electrodes as well as to prove the cleanliness of the system.[33] To demonstrate the well-known effect of specific adsorption of (bi)sulfate anions, which are often present in Nafion membranes after their pretreatment, cyclic voltammograms (CVs) in both perchloric acid and sulfuric acid solutions are also shown in Figure 1. The CV of the Pt(111) electrode in contact with 0.05 M H_2SO_4 reveals noticeable differences (Figure 1A). While the hydrogen adsorption and desorption processes (H_{upd}) in the potential region between 0.05 and ∼0.35 V are largely the same as in a 0.1 M $HClO_4$ solution, the adsorption of (bi)sulfate anions can be observed between 0.35 and 0.5 V as a reversible feature with a pair of sharp peaks at ∼0.52 V indicating the disorder/order phase transitions in the (bi)sulfate adsorbate layer.[34] A $(\sqrt{3} \times \sqrt{7})$R19.1° superstructure with co-adsorbed H_2O molecules is detected at the surface in the potential region between ∼0.52 and ∼0.8 V with an anion coverage of ∼0.2 ML as reported previously.[34] In addition, the CV demonstrates small peaks between 0.7 and 0.8 V. These features are likely to be associated with further rearrangements in the adsorbate layer as revealed, e.g., by electrochemical scanning tunneling microscopy.[34]

For further comparison, the Pt(111) electrodes modified with Nafion films were characterized in 0.1 M $HClO_4$ and 0.05 M H_2SO_4 solutions. The corresponding CVs recorded in 0.1 M $HClO_4$ reveal several characteristic features indicating that sulfonate groups, which are present in the Nafion polymer, adsorb on the Pt(111) surface. This observation is consistent with recent work by Subbaraman et al.[12] The hydrogen adsorption/desorption region between ∼0.05 and ∼0.35 V reveals no significant changes. However, in the potential region between ∼0.4 and ∼0.6 V, small characteristic peaks that have been assigned to the specific adsorption of sulfonates on Pt(111) appear.[34] Notably, the adsorption of sulfonate groups is apparently irreversible because of interactions between the sulfonate group and the interface described by the so-called "spring model".[13] This dramatically affects the adsorption/desorption of hydroxyl species in the potential region between ∼0.6 and ∼1.0 V (Figure 1A) as well as the ORR activity of the electrodes (Figure 1B). In 0.05 M H_2SO_4, adsorption of the sulfonate groups is likely masked or/and suppressed by the adsorbing (bi)sulfates coming from the supporting electrolyte. Therefore, the shape of the voltammogram characterizing the Nafion-covered Pt(111) electrode in 0.05 M H_2SO_4 is generally similar to that taken for the bare electrode in the same solution. However, a substantial difference is still noticeable; namely, the sharp peaks related to the disorder/order phase transition in the (bi)sulfate layer are suppressed.

Figure 1B compares RDE polarization curves for Pt(111) and Nafion-coated Pt(111) electrodes in 0.1 M $HClO_4$ and 0.05 M H_2SO_4 electrolytes. The effect of (bi)sulfate anions on the ORR activity of Pt(111) electrodes is well-known: significant ORR activity suppression is observed for the electrodes in 0.05 M H_2SO_4 solutions. This effect is largely associated with changes in Pt site availability due to competitive adsorption of (bi)sulfate anions from the supporting electrolyte.[35] As a result, a shift of ∼130 mV in the quasi-half-wave potential for ORR polarization curves is observed upon comparison of the unmodified Pt(111) electrodes in 0.1 M $HClO_4$ and 0.05 M H_2SO_4 (Figure 1B). The ORR curves taken for the Pt(111) and Nafion-coated Pt(111) electrodes in 0.05 M H_2SO_4 are very similar (Figure 1B), thus supporting the hypothesis that the effect of the sulfonate group in sulfuric acid is effectively masked by the adsorption of (bi)sulfate anions.[13,36] In contrast, a distinct cathodic shift of approx-

dx.doi.org/10.1021/cs501037y | ACS Catal. 2014, 4, 3772−3778

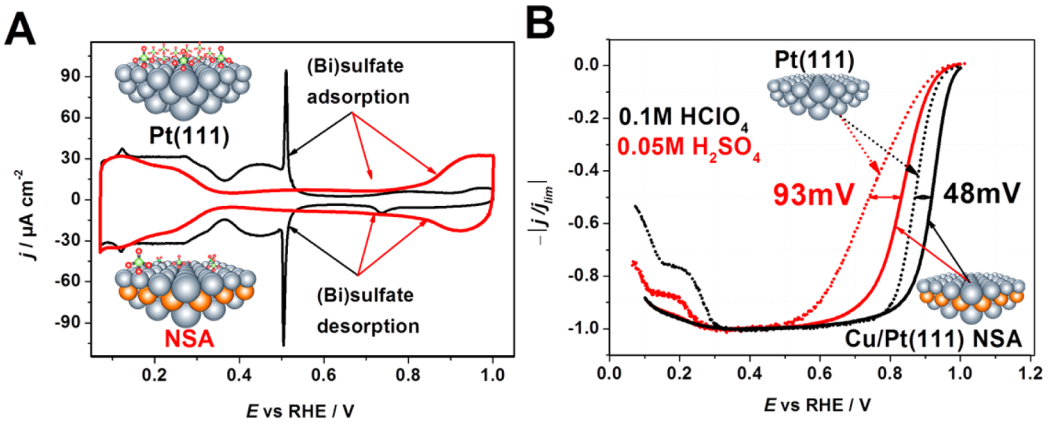

Figure 2. (A) Cyclic voltammograms characterizing the Pt(111) (black) and Cu/Pt(111) NSA (red) model electrodes in an Ar-saturated 0.05 M H_2SO_4 electrolyte. (B) Polarization curves characterizing the Pt(111) (···) and Cu/Pt(111) NSA (—) model electrodes in O_2-saturated 0.1 M $HClO_4$ (black) and 0.05 M H_2SO_4 (red), at 1600 rpm. dE/dt = 50 mV/s.

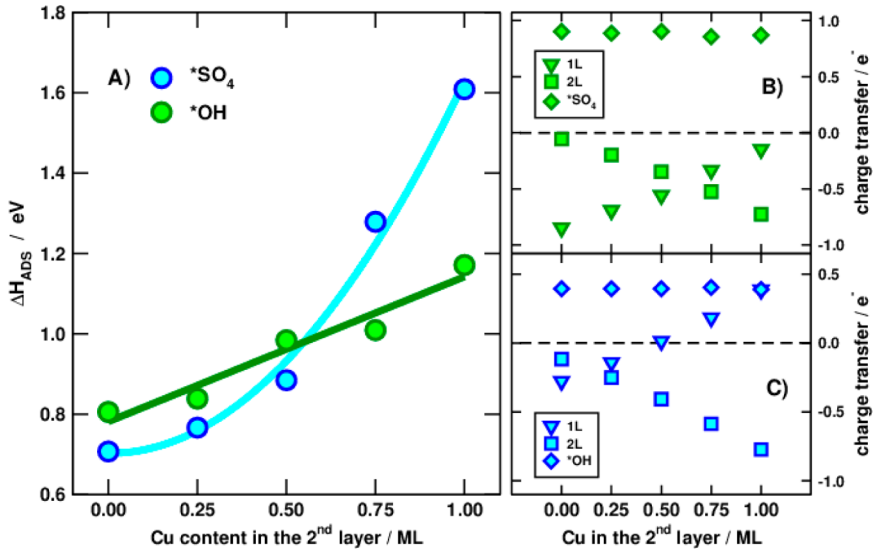

Figure 3. (A) Adsorption enthalpies for $*SO_4$ (blue) and *OH (green) on Pt(111) and Cu/Pt(111) NSA surfaces as a function of the Cu content in the subsurface layer. (B and C) Transfer of charge between the first layer (1L) and the second layers (2L) of the catalyst and the adsorbate for (B) $*SO_4$ and (C) *OH on Pt(111) and Pt/Cu NSAs. Negative and positive numbers indicate charge donation and withdrawal, respectively.

imately 23 mV in the half-wave potential is observed upon comparison of the Nafion-modified and bare Pt(111) electrodes in 0.1 M $HClO_4$ electrolytes (Figure 1B). However, the decrease in activity due to the adsorption of sulfonates is much smaller than the poisoning effect of (bi)sulfate anions.

The presence of copper atoms in the subsurface region of Pt(111) electrodes significantly changes their properties. Figure 2A shows the CVs of Pt(111) and Cu/Pt(111) NSA electrodes obtained in 0.05 M H_2SO_4. First, subsurface Cu atoms induce changes in the electronic structure of the surface, modifying H adsorption/desorption processes, which are in turn starting at substantially higher potentials at the Cu/Pt(111) NSA surface than at the Pt(111) surface, in agreement with previous results for this system.[37] Furthermore, the characteristic butterfly peaks at approximately ~0.5 V assigned to the (bi)sulfate adsorption/desorption process disappear completely for Cu/Pt(111) NSA electrodes. The shape of the voltammogram indicates that specific adsorption of (bi)sulfates is shifted toward more positive potentials (as indicated in Figure 2A). In our previous work, we found that the same integrated anodic charge for (bi)sulfate adsorption in the case of NSA can be reached only by applying approximately 1.0 V. However, *OH co-adsorption cannot be excluded in this potential region.

The changes in (bi)sulfate adsorption properties for the Cu/Pt(111) NSA and the consequential impact of this on the ORR activity have been explored via RDE measurements (Figure 2B). Generally, the Cu/Pt(111) NSA system demonstrates activity for the ORR higher than that of Pt(111) single crystals in 0.1 M $HClO_4$, expressed as a positive potential shift of ~48 mV in the pseudo-half-wave potentials between the corresponding polarization curves. In 0.05 M H_2SO_4, a positive anodic potential shift of ~93 mV is observed, representing one of the best reported performances for the ORR in H_2SO_4 (compare, e.g., with refs 38 and 39).

We performed DFT calculations to confirm and further quantify the changes in the adsorption energy of the (bi)sulfate species on NSAs. Figure 3A shows trends in adsorption enthalpies of $*SO_4$ and *OH as a function of the Cu content in the Pt subsurface region. Although in both cases the gradual addition of Cu decreases the adsorption enthalpies, the effect is qualitatively and quantitatively different: while the trend is roughly linear with a modest slope for *OH, the effect for $*SO_4$

dx.doi.org/10.1021/cs501037y | ACS Catal. 2014, 4, 3772−3778

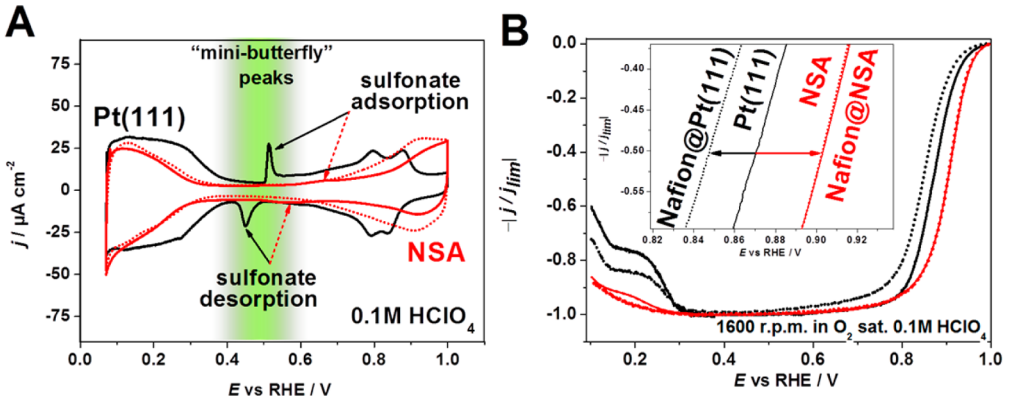

Figure 4. (A) Cyclic voltammograms characterizing Nafion-coated Pt(111) (black, solid line), Cu/Pt(111) NSA (red, dotted line), and Nafion-coated Cu/Pt(111) NSA (red, solid line) electrodes in Ar-saturated 0.1 M $HClO_4$. (B) Polarization curves characterizing the Pt(111) (black, solid line), Nafion-modified Pt(111) (black, dotted line), Cu/Pt(111) NSA (red, solid line) and Nafion-modified Cu/Pt(111) NSA (red, dotted line) model electrodes in 0.1 M $HClO_4$, at 1600 rpm. dE/dt = 50 mV/s.

is even more pronounced with an approximately parabolic trend. Besides, the maximal difference between the enthalpies of adsorption of *OH is ~0.37 eV, while it is ~0.90 eV in the case of $*SO_4$. Figure 3 also reveals another interesting fact: when the Cu content in the subsurface is below ~0.50 ML, the $*SO_4$ and *OH adsorption enthalpies are similar, which would suggest competitive adsorption when sulfate is in solution. However, for Cu coverages of more than ~0.50 ML, the adsorption of $*SO_4$ is dramatically suppressed as compared with that of *OH species favoring adsorption of the latter. It is thus possible to say that the weakening effect of subsurface Cu is greater on the adsorption energetics of $*SO_4$, and that the effect is more noticeable at high Cu coverages, which prevents the adsorption of sulfate on the NSAs, in agreement with the experimental results in Figures 1 and 2.

An explanation for the quantitatively and qualitatively dissimilar effect for *OH and sulfate adsorbates is given in panels B and C of Figure 3. These figures further characterize the transfer of charge between the adsorbates and the surface and subsurface layers of Pt(111) and the NSAs. Clearly, the charge transfer associated with the adsorption of *OH and $*SO_4$ is constant for all surfaces but strongly depends on the adsorbate: it is approximately equal to 0.4 e^- for *OH and 0.9 e^- for $*SO_4$. It is also clear from the figures that the relative charge distribution at the surface depends on both the nature of the adsorbates and the amount of Cu in the subsurface layer. With a certain degree of simplification, the situation can be described as follows. Because Cu has one more valence electron than Pt, the subsurface layer may act as an "electron reservoir". As the adsorption of SO_4^{2-} involves the more charge transfer than that of *OH, increasing the amount of Cu in the second layer would more significantly reduce the overall affinity of the surface for these adsorbates. In other words, the subsurface layer in Pt/Cu NSAs is rather electron-rich with respect to Pt(111), which causes the observed weaker binding of these adsorbates. Thus, the effect of subsurface Cu on Pt skins can be strongly correlated with charge transfer, which is in line with previous analyses of NSAs of Pt and transition metals,[40] the adsorption properties of which tend to follow simple electron counting rules.

To further illustrate the impact of the interactions between the sulfonate groups of the Nafion polymer on the activity of the Cu/Pt(111) NSA, Figure 4A shows the CVs of Pt(111) and Cu/Pt(111) NSA surfaces covered with Nafion in 0.1 M $HClO_4$. Although the hydrogen adsorption/desorption region remains almost unaffected for both systems, the voltammetric features in the potential region between ~0.4 and ~0.6 V related to the sulfonate adsorption on Pt(111) are heavily suppressed for the Cu/Pt(111) NSA sample. This suggests that the influence of the specific adsorption of sulfonate anions is much less pronounced. This is also supported by the DFT calculations showing that the adsorption energy of $CF_3CF_2SO_3$* (see schematics in Figure 5), used here to approximate the adsorption of Nafion sulfonate groups, on pure Pt(111) and on Pt(111) with 1 ML Cu in the subsurface region is ~0.3 eV weaker on the latter.

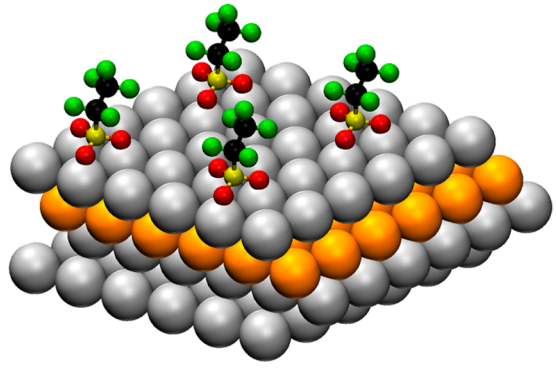

Figure 5. Schematics of $CF_3CF_2SO_3$* adsorption on *fcc* hollow sites on Pt(111) with 1 ML Cu in the subsurface layer (see the text for details).

Figure 4B shows polarization curves characterizing the effect of the Nafion film on the ORR activity of Pt(111) and Cu/Pt(111) NSAs. As has been already discussed, the presence of Nafion on Pt(111) hinders the ORR by blocking the active sites with the sulfonate groups adsorbed on the catalyst surface. As a consequence, a negative potential shift of ~23 mV in the electrode half-wave potential is observed. The electrocatalytic activity for Cu/Pt(111) NSA in 0.1 M $HClO_4$ increases compared with that with Pt(111) electrodes because of a weaker interaction between *OH species and the catalyst surface.[19] Interestingly, the polarization curves for the ORR on Cu/Pt(111) and Nafion-coated Cu/Pt(111) electrode in 0.1 M $HClO_4$ are almost identical. Figure 4B shows that the modification of Cu/Pt(111) NSA with Nafion has no

dx.doi.org/10.1021/cs501037y | ACS Catal. 2014, 4, 3772−3778

significant influence on ORR activity. This confirms that destabilization of the adsorbates by subsurface Cu has a beneficial effect largely by preventing or minimizing the poisoning effect related to important PEMFC electrolyte components.

4. CONCLUSIONS

PEM fuel cells mainly using Nafion membranes need to be made commercially viable through the development of more active and stable electrocatalysts under oxygen reduction reaction conditions. Ideal electrocatalysts should be tolerant toward poisoning with electrolyte species not directly involved in the ORR. For Nafion membranes, two common poisoning species are (bi)sulfates, which are often present in the membranes after their "activation" procedure, and sulfonate groups, which constitute the polymer itself. We have shown here that alloying Pt with monolayer amounts of Cu preferentially located in the subsurface layer of the catalyst has a 2-fold beneficial effect. On one hand, the catalytic activity toward the ORR is increased and remains the same in the presence of Nafion, and on the other hand, the tolerance of the catalyst toward (bi)sulfate and sulfonate groups is substantially enhanced. These two features of Cu/Pt(111) NSAs are due to peculiarities of the transfer of charge between the first two layers of the catalyst and the adsorbates, where Cu atoms in the second layer act as an electron reservoir for Pt top layers. This weakens the adsorption strength of adsorbates at the surface. The weakening effect is considerably larger for the (bi)sulfate species than for the key ORR intermediates, which is beneficial for the overall catalytic activity.

AUTHOR INFORMATION

Corresponding Author

*E-mail: bandarenka@ph.tum.de. Telephone: +49 89 289 12531.

Notes

The authors declare no competing financial interest.

ACKNOWLEDGMENTS

Financial support from the Cluster of Excellence RESOLV (EXC 1069) funded by the DFG (Deutsche Forschungsgemeinschaft) and in the framework of Helmholtz-Energie-Allianz "Stationäre elektrochemische Speicher und Wandler" (HA-E-0002) is gratefully acknowledged. F.C.-V. acknowledges funding from the EU's FP7/2007-2013 program, call FCH-JU-2011-1 under Grant n°303419, and thanks IDRIS, CINES (Project 609, GENCI/CT8), and PSMN for CPU time and assistance.

REFERENCES

(1) Wagner, F. T.; Lakshmanan, B.; Mathias, M. F. *J. Phys. Chem. Lett.* **2010**, *1*, 2204−2219.
(2) Gasteiger, H. A.; Kocha, S. S.; Sompalli, B.; Wagner, F. T. *Appl. Catal., B* **2005**, *56*, 9−35.
(3) Stephens, I. E. L.; Bondarenko, A. S.; Grønbjerg, U.; Rossmeisl, J.; Chorkendorff, I. *Energy Environ. Sci.* **2012**, *5*, 6744−6762.
(4) Ertl, G. *Angew. Chem., Int. Ed.* **2008**, *47*, 3524−3535.
(5) Koper, M. T. M. *Faraday Discuss.* **2008**, *140*, 11−24.
(6) Schnur, S.; Groß, A. *Catal. Today* **2011**, *165*, 129−137.
(7) Gasteiger, H. A.; Markovic, N. M. *Science* **2009**, *324*, 48−49.
(8) Gasteiger, H. A.; Garche, J. In *Handbook of Heterogeneous Catalysis*, 2nd ed.; Ertl, G., Knoezinger, H., Schueth, F., Weitkamp, J., Eds.; Wiley-CPH: Chichester, U.K., 2008; pp 3081−3120.
(9) Stamenkovic, V. R.; Fowler, B.; Mun, B. S.; Wang, G. F.; Ross, P. N.; Lucas, C. A.; Markovic, N. M. *Science* **2007**, *315*, 493−497.
(10) Stamenkovic, V.; Mun, B. S.; Mayrhofer, K. J. J.; Ross, P. N.; Markovic, N. M.; Rossmeisl, J.; Greeley, J.; Nørskov, J. K. *Angew. Chem., Int. Ed.* **2006**, *45*, 2897−2901.
(11) Ticianelli, E. A.; Derouin, C. R.; Srinivasan, S. *J. Electroanal. Chem.* **1988**, *251*, 275−295.
(12) Subbaraman, R.; Strmcnik, D.; Stamenkovic, V.; Markovic, N. M. *J. Phys. Chem. C* **2010**, *114*, 8414−8422.
(13) Subbaraman, R.; Strmcnik, D.; Paulikas, A. P.; Stamenkovic, V. R.; Markovic, N. M. *ChemPhysChem* **2010**, *11*, 2825−2833.
(14) Kodama, K.; Shinohara, A.; Hasegawa, N.; Shinozaki, K.; Jinnouchi, R.; Suzuki, T.; Hatanaka, T.; Morimoto, Y. *J. Electrochem. Soc.* **2014**, *161*, F649−F652.
(15) Bandarenka, A. S.; Koper, M. T. M. *J. Catal.* **2013**, *308*, 11−24.
(16) Stephens, I. E. L.; Bondarenko, A. S.; Bech, L.; Chorkendorff, I. *ChemCatChem* **2012**, *4*, 341−349.
(17) Tymoczko, J.; Schuhmann, W.; Bandarenka, A. S. *ChemElectroChem* **2014**, *1*, 213−219.
(18) Henry, J. B.; Maljusch, A.; Huang, M.; Schuhmann, W.; Bondarenko, A. S. *ACS Catal.* **2012**, *2*, 1457−1460.
(19) Tymoczko, J.; Schuhmann, W.; Bandarenka, A. S. *Phys. Chem. Chem. Phys.* **2013**, *15*, 12998−13004.
(20) Bondarenko, A. S.; Stephens, I. E. L.; Chorkendorff, I. *Electrochem. Commun.* **2012**, *23*, 33−36.
(21) Herrero, E.; Buller, L. J.; Abruna, H. D. *Chem. Rev.* **2001**, *101*, 1897−1930.
(22) Henry, J. B.; Maljusch, A.; Tymoczko, J.; Schuhmann, W.; Bandarenka, A. S. *Electrochim. Acta* **2013**, *112*, 887−893.
(23) Kresse, G.; Furthmüller, J. *Phys. Rev. B: Solid State* **1996**, *54*, 11169−11186.
(24) Perdew, J. P.; Burke, K.; Ernzerhof, M. *Phys. Rev. Lett.* **1997**, *78*, 1396.
(25) Kresse, G.; Joubert, D. *Phys. Rev. B: Solid State* **1999**, *59*, 1758−1775.
(26) Methfessel, M.; Paxton, A. T. *Phys. Rev. B: Solid State* **1989**, *40*, 3616−3621.
(27) Jinnouchi, R.; Hatanaka, T.; Morimoto, Y.; Osawa, M. *Phys. Chem. Chem. Phys.* **2012**, *14*, 3208−3218.
(28) Nørskov, J. K.; Rossmeisl, J.; Logadottir, A.; Lindqvist, L.; Kitchin, J. R.; Bligaard, T.; Jónsson, H. *J. Phys. Chem. B* **2004**, *108*, 17886−17892.
(29) Abild-Pedersen, F.; Greeley, J.; Studt, F.; Rossmeisl, J.; Munter, T. R.; Moses, P. G.; Skúlason, E.; Bligaard, T.; Nørskov, J. K. *Phys. Rev. Lett.* **2007**, *99*, 016105.
(30) Man, I. C.; Su, H.-Y.; Calle-Vallejo, F.; Hansen, H. A.; Martinez, J. I.; Inoglu, N. G.; Kitchin, J.; Jaramillo, T. F.; Norskov, J. K.; Rossmeisl, J. *ChemCatChem* **2011**, *3*, 1159−1165.
(31) Calle-Vallejo, F.; Koper, M. T. M. *Electrochim. Acta* **2012**, *84*, 3−11.
(32) Stephens, I. E. L.; Bondarenko, A. S.; Gronbjerg, U.; Rossmeisl, J.; Chorkendorff, I. *Energy Environ. Sci.* **2012**, *5*, 6744−6762.
(33) Berna, A.; Climent, V.; Feliu, J. M. *Electrochem. Commun.* **2007**, *9*, 2789−2794.
(34) Braunschweig, B.; Daum, W. *Langmuir* **2009**, *25*, 11112−11120.
(35) Markovic, N. M.; Gasteiger, H. A.; Ross, P. N. *J. Phys. Chem.* **1995**, *99*, 3411−3415.
(36) Strmcnik, D. S.; Tripkovic, D. V.; van der Vliet, D.; Chang, K. C.; Komanicky, V.; You, H.; Karapetrov, G.; Greeley, J.; Stamenkovic, V. R.; Markovic, N. M. *J. Am. Chem. Soc.* **2008**, *130*, 15332−15339.
(37) Stephens, I. E. L.; Bondarenko, A. S.; Perez-Alonso, F. J.; Calle-Vallejo, F.; Bech, L.; Johansson, T. P.; Jepsen, A. K.; Frydendal, R.; Knudsen, B. P.; Rossmeisl, J.; Chorkendorff, I. *J. Am. Chem. Soc.* **2011**, *133*, 5485−5491.
(38) Kuzume, A.; Herrero, E.; Feliu, J. M. *J. Electroanal. Chem.* **2007**, *599*, 333−343.
(39) Strmcnik, D.; Escudero-Escribano, M.; Kodama, K.; Stamenkovic, V. R.; Cuesta, A.; Marković, N. M. *Nat. Chem.* **2010**, *2*, 880−885.

(40) Calle-Vallejo, F.; Martínez, J. I.; García-Lastra, J. M.; Rossmeisl, J.; Koper, M. T. M. *Phys. Rev. Lett.* **2012**, *108*, 116103.